Platinum Diimine Bis(acetylide) Complexes: Synthesis, Characterization, and Luminescence Properties

Muriel Hissler,[†] William B. Connick,[†,‡] David K. Geiger,*[,§] James E. McGarrah,[†] Donald Lipa,[§] Rene J. Lachicotte,[†] and Richard Eisenberg*[,†]

Department of Chemistry, University of Rochester, Rochester, New York 14627-0216, and Department of Chemistry, State University of New York-College at Geneseo, Geneseo, New York 14454

Received October 25, 1999

A new set of luminescent platinum(II) diimine complexes has been synthesized and characterized. The anionic ligands in these complexes are arylacetylides. The complexes are brightly emissive in fluid solution with relative emission quantum yields ϕ_{em} ranging from 3×10^{-3} to 10^{-1}. Two series of complexes have been investigated. The first has the formula Pt(Rphen)($C{\equiv}CC_6H_5$)$_2$ where Rphen is 1,10-phenanthroline substituted in the 5-position with R = H, Me, Cl, Br, NO_2, or $C{\equiv}CC_6H_5$, while the second has the formula Pt(dbbpy)($C{\equiv}CC_6H_4X$)$_2$ where dbbpy = 4,4′-di(*tert*-butyl)bipyridine and X = H, Me, F, or NO_2. From NMR, IR, and electronic spectroscopies, all of the complexes are assigned a square planar coordination geometry with *cis*-alkynyl ligands. The crystal structure of Pt(phen)($C{\equiv}CC_6H_4CH_3$)$_2$ confirms this assignment. All of the complexes exhibit an absorption band at ca. 400 nm that corresponds to a Pt d $\rightarrow \pi^*_{diimine}$ charge-transfer transition. The variation of λ_{max} for this band with substituent variation supports this assignment. From similar changes in the energy of the solution luminescence as a function of substituents R and X, the emissive excited state is also of MLCT origin, but with spin-forbidden character on the basis of excited-state lifetime measurements (0.01−5.6 μs). The complexes undergo electron-transfer quenching, showing good Stern−Volmer behavior using 10-methylphenothiazine and *N*,*N*,*N*′,*N*′-tetramethylbenzidine as reductive quenchers. Excited-state reduction potentials are estimated on the basis of a simple thermochemical analysis. Crystal data for Pt(phen)($C{\equiv}CC_6H_4CH_3$)$_2$: monoclinic, space group *C*2/*c*, a = 19.0961(1) Å, b = 10.4498(1) Å, c = 11.8124(2) Å, β = 108.413(1)°, V = 2236.49 Å^3, number of reflections 1614, number of variables 150, R1 = 0.0163, wR2 ($I > 2\sigma$) = 0.0410.

Introduction

Complexes exhibiting excited-state properties consistent with a high degree of charge separation are of inherent interest for a number of reasons. One is their potential use in emerging technologies such as the design of molecular-scale electronic devices.[1−5] Another is their applicability in the design of supramolecular systems for the conversion of light energy to chemical energy.[3,6−15] Such systems will require components for collecting and funneling photon energy, electron−hole pair creation, charge separation by vectorial electron transfer, charge accumulation, and catalysis of the desired energy-storing reaction. The directional nature of charge-transfer excited states in square planar diimine complexes is ideal for electron−hole creation and separation, and consequently, these systems merit consideration for use in molecular photochemical devices and related supramolecular systems. The coordinative unsaturation of square planar complexes also renders them of interest for sensor applications.[16]

For more than a decade, platinum diimine complexes of the general formula Pt(diimine)X_2 have been known to be luminescent in fluid solution, with the energy and nature of the emitting state dependent on the anionic ligand X.[17−22] For the

[†] University of Rochester.
[‡] Present address: Department of Chemistry, University of Cincinnati, Cincinnati, OH 45221-0172.
[§] State University of New York-College at Geneseo.

(1) Ziessel, R. F. *J. Chem. Educ.* **1997**, *74*, 673−679.
(2) Balzani, V.; Moggi, L.; Scandola, F. In *Towards a Supramolecular Photochemistry: Assembly of Molecular Components to Obtain Photochemical Molecular Devices*; Balzani, V., Eds.; D. Reidel Publishing Co.: Dordrecht, Holland, 1987; pp 1−28.
(3) Balzani, V.; DeCola, L. In *Supramolecular Chemistry*; Balzani, V., DeCola, L., Eds.; Kluwer Academic Publishers: Dordrecht, Holland, 1992.
(4) Balzani, V. In *Supramolecular Photochemistry*; Balzani, V., Ed.; D. Reidel Publishing Co.: Dordrecht, Holland, 1987.
(5) Balzani, V.; Gomez-Lopez, M.; Stoddart, J. F. *Acc. Chem. Res.* **1998**, *31*, 405−414.
(6) Meyer, T. J. *Acc. Chem. Res.* **1989**, *22*, 163−170.
(7) Meyer, T. J. *Photochem. Energy Convers., Proc. Int. Conf. Photochem. Convers. Storage Solar Energy, 7th* **1989**, 75−95.
(8) Barbara, P. F.; Meyer, T. J.; Ratner, M. A. *J. Phys. Chem.* **1996**, *100*, 13148−13168.
(9) Meyer, T. J. *Abstr. Pap. Am. Chem. Soc.* **1996**, *212*, 222-INOR.
(10) Treadway, J. A.; Chen, P. Y.; Rutherford, T. J.; Keene, F. R.; Meyer, T. J. *J. Phys. Chem. A* **1997**, *101*, 6824−6826.
(11) Baxter, S. M.; Jones, J., W. E.; Danielson, E.; Worl, L.; Strouse, G.; Younathan, J.; Meyer, T. J. *Coord. Chem. Rev.* **1991**, *111*, 47−71.
(12) Yonemoto, E. H.; Riley, R. L.; Kim, Y. I.; Atherton, S. J.; Schmehl, R. H.; Mallouk, T. E. *J. Am. Chem. Soc.* **1992**, *114*, 8081−8087.
(13) Yonemoto, E. H.; Saupe, G. B.; Schmehl, R. H.; Hubig, S. M.; Riley, R. L.; Iverson, B. L.; Mallouk, T. E. *J. Am. Chem. Soc.* **1994**, *116*, 6, 4786−4795.
(14) Kaschak, D. M.; Mallouk, T. E. *Abstr. Pap. Am. Chem. Soc.* **1997**, *214*, 358-PHYS.
(15) Hasenknopf, B.; Hall, J.; Lehn, J. M.; Balzani, V.; Credi, A.; Campagna, S. *New J. Chem.* **1996**, *20*, 725−730.
(16) Kunugi, Y.; Mann, K. R.; Miller, L. L.; Exstrom, C. L. *J. Am. Chem. Soc.* **1998**, *120*, 589−590.
(17) Miskowski, V. M.; Houlding, V. H. *Inorg. Chem.* **1989**, *28*, 1529−1533.
(18) Miskowski, V. M.; Houlding, V. H.; Che, C.-M.; Wang, Y. *Inorg. Chem.* **1993**, *32*, 2518−2524.
(19) Kunkely, H.; Vogler, A. *J. Am. Chem. Soc.* **1990**, *112*, 5625−5627.

10.1021/ic991250n CCC: $19.00
Published on Web 01/20/2000

systems in which a dithiolate is the anion, the excited state has been assigned as a charge transfer from an orbital of mixed metal/dithiolate character to a π^* orbital localized on the diimine ligand.[23−25] For complexes in which X = CN, the emission is often structured and usually occurs at substantially higher energy, corresponding to a $^3(\pi\pi^*)$ excited state, although in more concentrated solutions, the di(cyanide) complexes exhibit a broad red-shifted excimeric emission.[20,26,27]

In 1994, Che published a brief account of a different luminescent platinum diimine complex in which X = phenylacetylide.[28] This complex, Pt(phen)(C≡CC$_6$H$_5$)$_2$, was said to be brightly emissive with an excited-state energy between those of the di(cyanide) and the dithiolate complexes, and a ^{3}MLCT emissive state was proposed. The bright luminescence and the change in excited state from those of the dithiolate and di(cyanide) complexes made this system and its derivatives worthy of further study. The notion of how different X ligands influence the relative positions of ligand-centered, ligand field, and charge-transfer excited states in platinum diimine complexes has been discussed by Miskowski et al.[18]

Luminescence in other platinum acetylide complexes has been noted as well.[29] The specific systems investigated were *trans*-Pt(C≡CR)$_2$(PEt$_3$)$_2$, where R = H or C$_6$H$_5$, and the luminescence of those systems was studied mainly in the solid state and frozen glass solutions at 77 K. While site heterogeneity was noted for the frozen glass samples, the emission was assigned as arising from a charge-transfer excited state involving Pt d_{z^2} and acetylenic π^* orbitals. In fluid solution, emission from the two acetylide complexes (R = H, C$_6$H$_5$) was described as "weak" and "barely above background".[29]

In this paper, we describe the synthesis, characterization, and luminescence properties of the highly emissive platinum diimine bis(arylacetylide) complexes. Through ligand variation, the nature of the excited state has been probed. The complexes are found to undergo electron-transfer quenching, and through the use of a simplified thermochemical cycle, excited-state reduction potentials are estimated. In the course of studying the photophysical properties of the Pt(diimine)(C≡CAr)$_2$ complexes, it was found that solution excited-state lifetimes decreased with increasing metal complex concentration indicative of self-quenching, which in turn has led to a separate investigation of self-quenching by platinum diimine complexes in general.[30] While the work described in this paper was in progress, a separate report by James et al. on the synthesis of the Pt(diimine)(C≡CAr)$_2$ complexes appeared.[31]

Experimental Section

Reagents. Phenanthroline (Aldrich) and K$_2$[PtCl$_4$] (Johnson Matthey) were used without further purification. Ethynylbenzene, 1-fluoro-4-ethynylbenzene, 1-methoxy-4-ethynylbenzene, and 4-ethynyltoluene (Aldrich) were used as received. 1-Nitro-4-ethynylbenzene,[32] 5-nitrophenanthroline,[33] Pt(phen)Cl$_2$,[34] and Pt(dbbpy)Cl$_2$[34] were prepared according to literature methods. Pt(Xphen)Cl$_2$ complexes, where X is NO$_2$, Cl, CH$_3$, or Br in the 5-position of phenanthroline, were prepared in a fashion analogous to the synthesis of Pt(phen)Cl$_2$.[34] The syntheses of Pt(Rphen)(alkynyl)$_2$ complexes were performed under nitrogen with all solvents degassed prior to use.

5-Bromophenanthroline (Brphen). The compound was synthesized using a modification of the preparation described by Mlochowski.[35] The yield of product is quite sensitive to the amount of bromine employed, the temperature, and the reaction time. Higher temperatures result in the formation of varying amounts of 5,6-dibromophenanthroline and 1,10-phenanthroline-5,6-dione. In our hands, the following preparation resulted in the maximum yield of product. A 3.6 g (20 mmol) sample of phenanthroline was placed in a heavy-walled glass reaction tube with a Teflon screw top fitted with a Viton O-ring. The reaction vessel was placed in an ice bath, and 12 mL of oleum (15%) and 0.60 mL (11.6 mmol) of bromine were added. The reaction tube was placed in a silicon oil bath, and the temperature was slowly raised to 135 °C. After 23 h, the reaction mixture was cooled to room temperature, poured over ice, and neutralized with NH$_4$OH. The mixture was extracted with CHCl$_3$. The extracts were stirred with charcoal and then dried over Na$_2$SO$_4$. The crude reaction mixture contained about 5% unreacted phenanthroline as judged by ^{1}H NMR spectroscopy. The solid was recrystallized from hot diethyl ether with a minimum amount of CH$_2$Cl$_2$. Yield: 4.67 g (90%). ^{1}H NMR (CDCl$_3$): δ 9.17 (m, 2H), 8.64 (dd, 1H, J = 8.0 Hz, J = 1.6 Hz), 8.15 (pseudo-dd, 1H, J = 8.4 Hz, J = 2.0 Hz, J = 8.0 Hz, J = 1.6 Hz), 8.12 (s, 1H), 7.72 (dd, 1H, J = 8.4 Hz, J = 4.0 Hz), 7.61 (dd, 1H, J = 8.0 Hz, J = 4.4 Hz).

Pt(phen)(C≡CC$_6$H$_5$)$_2$ (1). A 100 mg (0.22 mmol) sample of Pt(phen)Cl$_2$, 10 mg of CuI, 0.2 mL (2.0 mmol) of phenylacetylene, 4 mL of DMF, and 3 mL of diethylamine were sonicated for 4 h. The flask was chilled, and the bright yellow precipitate was collected by filtration and washed with ether. The material was recrystallized from methylene chloride and methanol. Yield: 100 mg (77%). ^{1}H NMR (DMSO-d_6): δ 9.71 (2H, d, J = 5.2 Hz), 9.04 (2H, d, J = 8.0 Hz), 8.30 (2H, s), 8.23 (2H, dd, J = 8.4 Hz, J = 5.2 Hz), 7.51 (4H, d, J = 7.2 Hz), 7.32 (4H, pseudo-t, J = 7.2 Hz, J = 7.6 Hz), 7.22 (2H, pseudo-t, J = 7.6 Hz, J = 7.2 Hz). FT-IR (mull): ν/cm^{-1} 2106, 2116 ($\nu_{C\equiv C}$). FAB$^+$ (*m*-NBA): *m*/*z* 578.0 [M + H]$^+$. UV−vis (CH$_3$CN): λ_{max}/nm (ϵ/M^{-1} cm^{-1}) 392 (8000), 292 (sh) (32 400), 270 (51 000). Anal. Calcd for C$_{28}$H$_{18}$N$_2$Pt (M_r = 577.54): C, 58.23; H, 3.14; N, 4.85. Found: C, 57.95; H, 2.90; N, 4.80.

Pt(phen)(C≡CC$_6$H$_4$CH$_3$)$_2$ (2). The procedure followed for **1** was used except that 0.22 mL of ethynyltoluene was used. Yield: 120 mg (88%). ^{1}H NMR (DMSO-d_6): δ 9.83 (2H, dd, J = 5.1 Hz, J = 1.2 Hz), 9.04 (2H, dd, J = 8.2 Hz, J = 1.3 Hz), 8.32 (2H, s), 8.25 (2H, dd, J = 8.3 Hz, J = 5.2 Hz), 7.22 (AB quartet, 8H, J_{AB} = 8.0 Hz, $\Delta\nu$ = 56.9 Hz), 2.31 (6H, s). FT-IR (mull): ν/cm^{-1} 2110, 2120 (sh) ($\nu_{C\equiv C}$). FAB$^+$ (*m*-NBA): *m*/*z* 606.0 [M + H]$^+$. UV−vis (CH$_3$CN): λ_{max}/nm (ϵ/M^{-1} cm^{-1}): 392 (9800), 292 (sh) (46 400), 270 (70 500). Anal. Calcd for C$_{30}$H$_{22}$N$_2$Pt·0.5 CH$_3$OH (M_r = 605.55 + 16.02): C, 58.93; H, 3.89; N, 4.51. Found: C, 59.03; H, 3.66; N, 4.66.

Pt(phen)(C≡CC$_6$H$_4$F)$_2$ (3). The procedure followed for **1** was used except that 0.18 mL of 1-ethynyl-4-fluorobenzene was used. Yield: 100 mg (91%). ^{1}H NMR (DMSO-d_6): δ 9.79 (2H, d, J = 5.4 Hz), 9.05 (2H, d, J = 8.4 Hz), 8.31 (2H, s), 8.24 (2 H, dd, J = 8.4 Hz, J = 5.4 Hz), 7.46 (4H, dd, J = 8.4 Hz, J = 5.7 Hz), 7.15 (4H, t, J = 9.0 Hz). FT-IR (mull): ν/cm^{-1} 2112, 2123 (sh) ($\nu_{C\equiv C}$). FAB$^+$ (*m*-NBA): *m*/*z* 614 [M + H]$^+$. UV−vis (CH$_3$CN): λ_{max}/nm (ϵ/M^{-1} cm^{-1}) 391 (7100), 286 (sh) (29 600), 265 (46 800). Anal. Calcd for

(20) Wan, K.-T.; Che, C.-M.; Cho, K.-C. *J. Chem. Soc., Dalton Trans.* **1991**, 1077−1080.
(21) Zuleta, J. A.; Chesta, C. A.; Eisenberg, R. *J. Am. Chem. Soc.* **1989**, *111*, 8916−8917.
(22) Zuleta, J. A.; Bevilacqua, J. M.; Eisenberg, R. *Coord. Chem. Rev.* **1992**, *111*, 237−248.
(23) Cummings, S. D.; Eisenberg, R. *J. Am. Chem. Soc.* **1996**, *118*, 1949−1960.
(24) Zuleta, J. A.; Bevilacqua, J. M.; Proserpio, D. M.; Harvey, P. D.; Eisenberg, R. *Inorg. Chem.* **1992**, *31*, 2396−2404.
(25) Cummings, S. D.; Eisenberg, R. *Inorg. Chem.* **1995**, *34*, 2007−2014.
(26) Che, C.-M.; Wan, K.-T.; He, L.-Y.; Poon, C.-K.; Yam, V. W.-W. *J. Chem. Soc., Chem. Commun.* **1989**, 943−945.
(27) Kunkely, H.; Vogler, A. *J. Am. Chem. Soc.* **1990**, *112*, 5625−5627.
(28) Chan, C.-W.; Cheng, L.-K.; Che, C.-M. *Coord. Chem. Rev.* **1994**, *132*, 87−97.
(29) Sacksteder, L.; Baralt, E.; DeGraff, B. A.; Lukehart, C. M.; Demas, J. N. *Inorg. Chem.* **1991**, *30*, 2468−2476.
(30) Connick, W. B.; Geiger, D. P.; Eisenberg, R. *Inorg. Chem.* **1999**, *38*, 3264−3265.
(31) James, S. L.; Younus, M.; Raithby, P. R.; Lewis, J. *J. Organomet. Chem.* **1997**, *543*, 233−235.
(32) Takahashi, S.; Kuroyama, Y.; Sonogashira, K.; Hagihara, N. *Synthesis* **1980**, 627−630.
(33) Smith, G. F.; Cagle, J., F. W. *J. Org. Chem.* **1947**, *12*, 781−784.
(34) Hodges, K. D.; Rund, J. V. *Inorg. Chem.* **1975**, *14*, 525−528.
(35) Mlochowski, J. *Roczniki Chem., Ann. Soc. Chim. Polonorum* **1974**, *48*, 2145.

$C_{28}H_{16}N_2F_2Pt$ (M_r = 613.52): C, 54.82; H, 2.63; N, 4.57. Found: C, 54.64; H, 2.56; N, 4.59.

Pt(NO_2phen)(C≡CC_6H_5)$_2$ (4). Method 1: To 100 mg (0.20 mmol) of Pt(phenNO_2)Cl_2 and 10 mg of CuI were added 4 mL of DMF, 4 mL of triethylamine, and 0.2 mL of ethynylbenzene. The mixture was sonicated for $3^1/_2$ h, during which time most of the starting material dissolved. The solution was filtered, removing ca. 10 mg of yellow solid identified as starting material. The product was isolated from the filtrate with the addition of diethyl ether and dried under vacuum. Yield: 96 mg (76%). Method 2: A 50 mg (0.102 mmol) sample of Pt(5-NO_2phen)Cl_2 and 1 mg of CuI were placed in a Schlenk flask under nitrogen. A mixture of dichloromethane (20 mL), acetonitrile (10 mL), and diisopropylamine (3 mL) was degassed and added to the flask. Then 0.03 mL of ethynylbenzene was added to the mixture, which was stirred for 24 h at room temperature. The solvent was removed under vacuum. The crude precipitate was chromatographed on neutral alumina using dichloromethane/methanol as eluent with a gradient of methanol (0−10, v/v). The product was further purified by recrystallization from acetone/hexane. Yield: 39 mg (61%). ^{1}H NMR (DMSO-d_6): δ 9.82 (d, 2H, J = 4.5 Hz), 9.39 (s, 1H), 9.36 (d, 1H, J = 9.3 Hz), 9.24 (d, 1H J = 7.8 Hz), 8.34 (m, 2H), 7.42 (d, 4H, J = 7.5 Hz), 7.32 (pseudo-t, 4H, J = 7.2 Hz, J = 7.7 Hz), 7.21 (pseudo-t, 2H, J = 7.2 Hz). FT-IR (mull): ν/cm^{-1} 2116, 2126 (sh) ($\nu_{C\equiv C}$); 842, 1334, 1484 (ν_{NO_2}). FAB$^+$ (*m*-NBA) *m*/*z*: 623 [M + H]$^+$. UV−vis (CH_3CN): λ_{max}/nm (ϵ/M^{-1} cm^{-1}) 397 (5000), 323 (sh) (6200), 272 (31 000). Anal. Calcd for $C_{28}H_{17}N_3O_2Pt\cdot C_3H_6O$ (M_r = 622.54 + 58.08): C, 54.71; H, 3.41; N, 6.17. Found: C, 54.63; H, 3.23; N, 6.31.

Pt(Brphen)(C≡CC_6H_5)$_2$ (5). A 100 mg (0.15 mmol) sample of Pt(Brphen)Cl_2 and 10 mg of CuI were placed in a round-bottom flask under nitrogen. A mixture of 4 mL of DMF and 3 mL of Et_3N was degassed and added to the flask. A 2 mL portion of ethynylbenzene was added to the mixture, which was sonicated for 3 h. After filtration, the remaining Et_3N was removed under vacuum. The DMF solution was added to CH_2Cl_2 and extracted with water. The CH_2Cl_2 fraction was washed with water and then evaporated to dryness. Yield: 69 mg (86%). The NMR spectrum of the material showed a small amount of starting material; the sample was purified by preparative TLC (silica gel; 1% MeOH/CH_2Cl_2). ^{1}H NMR (DMSO-d_6): δ 9.77 (d, 1H, J = 5.2 Hz), 9.70 (d, 1H, J = 4.8 Hz), 8.99 (d, 1H, J = 8.4 Hz), 8.92 (d, 1H, J = 8.4 Hz), 8.74 (s, 1H), 8.28 (dd, 1H, J = 8.0 Hz, J = 5.2 Hz), 8.19 (dd, 1H, J = 8.4 Hz, J = 5.4 Hz), 7.41 (m, 4H), 7.31 (pseudo-t, 4H, J = 7.6 Hz), 7.20 (pseudo-t, 2H, J = 7.2 Hz). FT-IR (mull): ν/cm^{-1} 2116, 2125 (sh) ($\nu_{C\equiv C}$). FAB$^+$ (*m*-NBA): *m*/*z* 656 [M + H]$^+$. UV−vis (CH_3CN): λ_{max}/nm (ϵ/M^{-1} cm^{-1}) 395 (8000), 262 (86 000). Anal. Calcd for $C_{28}H_{17}N_2PtBr$ (M_r = 656.44): C, 51.23; H, 2.61; N, 4.27. Found: C, 50.94; H, 2.71; N, 4.09.

Pt(Clphen)(C≡CC_6H_5)$_2$ (6). The procedure for Pt(Brphen)-(C≡CC_6H_5)$_2$ was followed except that 132 mg (0.275 mmol) of Pt(Clphen)Cl_2 and 10 mL of degassed MeCN were added to the reaction mixture. Yield: 116 mg (69%). ^{1}H NMR (DMSO-d_6): δ 9.85 (d, 1H, J = 4.8 Hz), 9.75 (d, 1H, J = 4.8 Hz), 9.12 (d, 1H, J = 8.4 Hz), 8.95 (d, 1H, J = 8.0 Hz), 8.61 (s, 1H), 8.33 (dd, 1H, J = 8.4 Hz, J = 5.2 Hz), 8.23 (dd, 1H, J = 8.0 Hz, J = 5.2 Hz), 7.42 (m, 4H), 7.31 (pseudo-t, 4H, J = 7.6 Hz), 7.19 (pseudo-t, 2H, J = 7.6 Hz). FT-IR (mull): ν/cm^{-1} 2121, 2130 (sh) ($\nu_{C\equiv C}$). FAB$^+$ (*m*-NBA): *m*/*z* 612 [M + H]$^+$. UV−vis (CH_3CN): λ_{max}/nm (ϵ/M^{-1} cm^{-1}) 397 (7200), 272 (49 500). Anal. Calcd for $C_{28}H_{17}N_2ClPt\cdot CH_3OH$ (M_r = 611.98 + 32.04): C, 54.08; H, 3.29; N, 4.35. Found: C, 54.46; H, 2.95; N, 4.32.

Pt(CH_3phen)(C≡CC_6H_5)$_2$ (7). The procedure for **6** was followed except 70.0 mg (0.152 mmol) of Pt(CH_3phen)Cl_2 was used. Yield: 57.6 mg (64%). ^{1}H NMR (DMSO-d_6): δ 9.81 (d, 1H, J = 5.1 Hz), 9.71 (d, 1H, J = 5.1 Hz), 9.06 (d, 1H, J = 8.5 Hz), 8.88 (d, 1H, J = 8.3 Hz), 8.24 (dd, 1H, J = 8.4 Hz, J = 5.2 Hz) 8.17 (dd, 1H, J = 8.2 Hz, J = 5.2 Hz), 8.10 (s, 1H), 7.41 (m, 4H), 7.31 (m, 4H), 7.19 (m, 2H), 2.87 (s, 3H). FT-IR (mull): ν/cm^{-1} 2117, 2126 (sh). FAB$^+$ (*m*-NBA): *m*/*z* 592 [M + H]$^+$. UV−vis (CH_3CN) λ_{max}/nm (ϵ/M^{-1} cm^{-1}) 396 (7600), 272 (49 400). Anal. Calcd for $C_{29}H_{20}N_2Pt\cdot H_2O$ (M_r = 591.57 + 18.02): C, 57.14; H, 3.64; 4.60. Found: C, 56.88; H, 3.44; N, 4.65.

Pt(C_6H_5C≡Cphen)(C≡CC_6H_5)$_2$ (8). A 140 mg (0.27 mmol) sample of Pt(Brphen)Cl_2, 16 mg of Pd(PPh_3)$_2Cl_2$, and 2 mg of CuI were placed in a round-bottom flask under nitrogen. A mixture of 5 mL of DMF and 3 mL of Et_3N was deaerated and added to the flask. A 44 μL (0.40 mmol) portion of ethynylbenzene was added to the mixture, which was stirred at room temperature for 2 h. After filteration, the remaining Et_3N base was removed via rotary evaporation and the DMF solvent was removed under vacuum. The golden residue was recrystallized from $CHCl_3$ and EtOH. A 120 mg sample of material was collected. A bright yellow fraction was isolated by preparative TLC (silica gel; 1% MeOH/CH_2Cl_2). Yield: 45 mg (25%). ^{1}H NMR (DMSO-d_6): δ 9.89 (d, 1H, J = 5.2 Hz), 9.80 (d, 1H, J = 5.2 Hz), 9.30 (dd, 1H, J = 8.4 Hz, J = 1.2 Hz), 9.01 (d, 1H, J = 8.4 Hz), 8.65 (s, 1H), 8.35 (dd, 1H, J = 8.4 Hz, J = 5.2 Hz), 8.25 (dd, 1H, J = 8.4 Hz, J = 5.2 Hz), 7.84 (m, 2H), 7.54 (m, 3H), 7.43 (m, 4H), 7.31 (t, 4H, J = 7.6 Hz), 7.20 (pseudo-t, 2H, J = 8.0 Hz, J = 7.2 Hz). FT-IR (mull): ν/cm^{-1} 2106, 2115, 2124 ($\nu_{C\equiv C}$). FAB$^+$ (*m*-NBA): *m*/*z* 677 [M]$^+$. UV−vis (CH_3CN): λ_{max}/nm (ϵ/M^{-1} cm^{-1}) 396 (9600), 336 (23 600), 273 (66 500). Anal. Calcd for $C_{36}H_{22}N_2Pt\cdot CH_3OH$ (M_r = 677.66 + 32.04): C, 62.62; H, 3.69; N, 3.95. Found: C, 62.71; H, 3.47; N, 4.02.

Pt(dbbpy)(C≡CC_6H_5)$_2$ (9). A 150 mg (0.28 mmol) sample of Pt(dbbpy)Cl_2 and 5 mg of CuI were placed in a Schlenk flask under nitrogen. A solution of 15 mL of dichloromethane and 5 mL of diisopropylamine was degassed and added to the flask. Ethynylbenzene (0.08 mol) was then added to the mixture, which was stirred for 24 h at room temperature. The solvent was removed under vacuum. The crude precipitate was chromatographed on neutral alumina using hexane/dichloromethane as eluent with a gradient of dichloromethane (20−100, v/v). The yellow product was further purified by recrystallization from dichloromethane/methanol and hexane. Yield: 110 mg (58%). R_f = 0.50 (20 vol % hexane in dichloromethane, silica gel).^{1}H NMR (d_6-acetone): δ 9.66 (d, 2H, J = 6 Hz), 8.61 (d, 2H, J = 1 Hz), 7.86 (dd, 2H, J = 6 Hz, J = 2 Hz), 7.38 (dd, 4H, J = 8 Hz), 7.23 (t, 4H, J = 8 Hz), 7.11 (t, 2H, J = 8 Hz), 1.46 (s, 18H). FT-IR (KBr): ν/cm^{-1} 2119, 2106 ($\nu_{C\equiv C}$). FAB$^+$ (*m*-NBA): *m*/*z* 666 [M + H]$^+$. UV−vis (CH_3CN): λ_{max}/nm (ϵ/M^{-1} cm^{-1}) 386 (5800), 281 (sh) (42 200), 262 (44 300). Anal. Calcd for $C_{34}H_{34}N_2Pt\cdot CH_3OH$ (M_r = 665.73 + 32.04): C, 60.25; H, 5.49; N, 4.01. Found: C, 60.43; H, 5.44; N, 3.83.

Pt(dbbpy)(C≡$CC_6H_4CH_3$)$_2$ (10). The procedure followed for **9** was used except that 0.09 mL of ethynyltoluene was used. Yield: 120 mg (61%). R_f = 0.51 (20 vol % hexane in dichloromethane, silica gel). ^{1}H NMR ($CDCl_3$): δ 9.53 (d, 2H, J = 5 Hz), 7.89 (d, 2H, J = 2 Hz), 7.40 (dd, 2H, J = 6 Hz, J = 2 Hz), 7.15 (AB quartet, 8H, J_{AB} = 8.0 Hz, $\Delta\nu$ = 139.8 Hz), 2.41 (s, 6H), 1.34 (s, 18H). FT-IR (KBr): ν/cm^{-1} 2112, 2124 (sh) ($\nu_{C\equiv C}$). FAB$^+$ (*m*-NBA): *m*/*z* 693 [M + H]$^+$. UV−vis (CH_3CN): λ_{max}/nm (ϵ/M^{-1} cm^{-1}) 389 (8200), 273 (73 000). Anal. Calcd for $C_{36}H_{38}N_2Pt$ (M_r = 693.79): C, 62.32; H, 5.52; N, 4.04. Found: C, 62.28; H, 5.64; N, 3.80.

Pt(dbbpy)(C≡$CC_6H_4OCH_3$)$_2$ (11). The procedure followed for **9** was used except that 0.09 mL of 1-methoxy-4-ethynylbenzene was used. Yield: 130 mg (64%). R_f = 0.48 (dichloromethane, silica gel). ^{1}H NMR (d_6-acetone): δ 9.68 (d, 2H, J = 6 Hz), 8.59 (d, 2H, J = 1.6 Hz), 7.84 (dd, 2H, J = 5.6 Hz, J = 1.6 Hz), 7.06 (AB quartet, 8H, J_{AB} = 8.8 Hz, $\Delta\nu$ = 196.2 Hz), 3.77 (s, 6 H), 1.46 (s, 18H). FT-IR (KBr): ν/cm^{-1} 2111, 2121 (sh) ($\nu_{C\equiv C}$). FAB$^+$ (*m*-NBA): *m*/*z* 725 [M + H]$^+$. UV−vis (CH_3CN): λ_{max}/nm (ϵ/M^{-1} cm^{-1}) 393 (6600), 279 (38 000). Anal. Calcd for $C_{36}H_{38}N_2PtO_2\cdot CH_3OH$ (M_r = 725.79 + 32.04): C, 58.64; H, 5.59; N, 3.70. Found: C, 58.46; H, 5.57; N, 3.31.

Pt(dbbpy)(C≡CC_6H_4F)$_2$ (12). The procedure followed for **9** was used except that 0.08 mL of 1-fluoro-4-ethynylbenzene was used. Yield: 146 mg (74%). R_f = 0.61 (20 vol % hexane in dichloromethane, silica gel). ^{1}H NMR (d_6-acetone): δ 9.61 (d, 2H, J = 6 Hz), 7.88 (s, 2H), 7.51 (d, 2H, J = 6 Hz), 7.41 (dd, 4 H, J = 8.0 Hz, J = 5.6 Hz), 6.86 (pseudo-t, 4 H, J = 8.8 Hz) 1.38 (s, 18H). FT-IR (KBr): ν/cm^{-1} 2114, 2126 (sh) ($\nu_{C\equiv C}$). FAB$^+$ (*m*-NBA): *m*/*z* 701 [M + H]$^+$. UV−vis (CH_3CN) λ_{max}/nm (ϵ/M^{-1} cm^{-1}) 385 (7500), 271 (55 800). Anal. Calcd for $C_{34}H_{32}N_2PtF_2\cdot 0.5\ CH_2Cl_2$ (M_r = 701.71 + 42.47): C, 55.68; H, 4.47; N, 3.76. Found: C, 55.63; H, 4.80; N, 3.43.

Pt(dbbpy)(C≡$CC_6H_4NO_2$)$_2$ (13). The procedure followed for **9** was used except that 0.100 mg (0.57 mmol) of 1-nitro-4-ethynylbenzene was used. Yield: 139 mg (61%). R_f = 0.81 (10 vol % hexane in dichloromethane, silica gel). ^{1}H NMR($CDCl_3$): δ 9.50 (d, 2H, J = 6.2 Hz), 7.94 (d, 2H, J = 2.0 Hz), 7.58 (dd, 2H, J = 6.2 Hz, J = 2.0 Hz), 7.80 (AB quartet, 8 H, J_{AB} = 9.1 Hz, $\Delta\nu$ = 214.2 Hz), 1.41 (s, 18H).

Table 1. Crystallographic Data for Pt(phen)(C≡$CC_6H_4CH_3$)$_2$ (**2**)

empirical formula	$C_{30}H_{22}N_2Pt$	abs correction	empirical (SADABS)
fw	605.59	transm range	0.633−0.928
T, K	193(2)	F(000)	1176
λ, Å	0.710 73	2θ range, deg	5.5 to 46.8
cryst syst	monoclinic	limiting indices	$-21 \le h \le 19$
space group	$C2/c$ (no. 15)		$-11 \le k \le 10$
Z	4		$-12 \le l \le 13$
a, Å[a]	19.0961(1)	no. of reflns collected	4857
b, Å[a]	10.4498(1)	no. of independent/obsd ($I > 2\sigma$) reflns	1614/1574
c, Å[a]	11.8124(2)	no. of data/restraints/params	1614/0/150
β, deg[a]	108.413(1)	goodness of fit[b]	1.088
V, Å^3	2236.49	R1, wR2 ($I > 2\sigma$)[c]	0.0163, 0.0410
ρ_{calcd}, g cm^{-3}	1.799	R1, wR2 (all data)[c]	0.0170, 0.0413
μ, mm^{-1}	6.295	largest difference peak and hole, e/Å^3	0.584 and −0.603

[a] It has been noted that the integration program SAINT produces cell constant errors that are unreasonably small, since systematic error is not included. More reasonable errors might be estimated at 10× the listed value. [b] GOF = $[\Sigma[w(F_o^2 - F_c^2)^2]/(n-p)]^{1/2}$, where n and p denote the number of data and parameters, respectively. [c] $R_1 = (\Sigma||F_o| - |F_c||)/\Sigma|F_o|$; wR2 = $[\Sigma[w(F_o^2 - F_c^2)^2]/\Sigma[w(F_o^2]]^{1/2}$, where $w = 1/[\sigma^2(F_o^2) + (aP)^2 + bP]$ and $P = f(\max)$ or $F_o^2 + (1-f)F_c^2$.

FT-IR (KBr): ν/cm^{-1} 2111, 2121 (sh) ($\nu_{C\equiv C}$) 852, 1337, 1504 (ν_{NO_2}). FAB$^+$ (*m*-NBA): *m*/*z* 756 [M + H]$^+$. UV−vis (CH_3CN): λ_{max}/nm (ϵ/M^{-1} cm^{-1}) 371 (38 100), 320 (26 800), 278 (19 600). Anal. Calcd for $C_{34}H_{32}N_4PtO_4 \cdot 2CH_3OH$ (M_r = 755.73 + 64.08): C, 52.74; H, 4.92; N, 6.83. Found: C, 52.58; H, 4.53; N, 6.52.

Physical Measurements. Infrared spectra were obtained from tetrachloroethylene mulls using a Perkin-Elmer 1600 FTIR spectrometer or from KBr pellets using a Mattson Galaxy 6020 FTIR spectrometer. ^{1}H NMR spectra were recorded on a Bruker AMX-400 or DPX 300 spectrometer (400 and 300 MHz, respectively). Cyclic voltammetry experiments were carried out on either a BAS CV-37 electrochemical analyzer or an EG&G PAR 263A potentiostat/galvanostat using a three-electrode single-cell compartment. All samples were degassed with nitrogen or argon. A Pt working electrode, Pt auxiliary electrode, and $Ag/AgNO_3$/acetonitrile reference electrode were used. For all of the measurements, the ferrocene/ferrocenium couple at 0.40 V vs NHE was used to calibrate the cell potential.

Absorption spectra were recorded using either a Hewlett-Packard HP8452A or a Hitachi U2000 spectrometer. Luminescence spectra were obtained using a Spex Fluorolog-2 spectrophotometer and corrected for instrumental response. Fluid solution emission samples were freeze−pump−thaw cycled at least four times with a vacuum of 10^{-4} Torr or lower. Frozen glass emission samples at 77 K were prepared by inserting a 3 mm (internal diameter) quartz tube containing a ca. 10^{-5} M solution (butyronitrile or ethanol/methanol (3:1)) of the complex into a quartz-tipped finger dewar of liquid nitrogen. Luminescence quantum yields were referenced to tris(2,2′-bipyridyl)ruthenium(II) in acetonitrile (Φ = 0.062),[36] as previously described.[37] Long emission lifetimes were measured using an excimer pumped dye laser system (1−3 mJ/pulse) and fitted to single-exponential decays.[38] Shorter luminescent lifetimes were determined using time-correlated single-photon counting.[39]

For all the compounds studied, unless otherwise noted, self-quenching was observed.[30] Over a range of concentrations (5×10^{-6} to approximately 2×10^{-4} M), the emission decays ($k_{obs} = 1/\tau$) are well modeled by a modified Stern−Volmer expression (eq 1),

$$k_{obs} = k_q[Pt] + k_o \quad (1)$$

where k_q is the self-quenching rate constant, [Pt] is the concentration of Pt complex, and k_o ($1/\tau_o$) is the rate of excited-state decay at infinite dilution. For the self-quenching studies, k_{obs} values at each concentration were taken at the emission maximum or at higher energy and averaged. Bimolecular reductive quenching studies were performed by luminescence lifetime measurements and fit by Stern−Volmer kinetics (eq 2),

$$\tau_o/\tau = 1 + k_q\tau_o[\text{quencher}] \quad (2)$$

where k_q is the quenching rate constant, [quencher] is the concentration of quencher, and τ_o and τ are the lifetimes of the chromophore in the absence and presence of quencher, respectively. The concentration of Pt chromophore used in these studies was held constant at ca. 3×10^{-5} M, while quencher concentrations varied in the range 5×10^{-6} to 3×10^{-4} M. *N*,*N*,*N*′,*N*′-Tetramethylbenzidine (TMB) was sublimed just prior to use.

Crystal Structure Determination of Pt(phen)(C≡$CC_6H_4CH_3$)$_2$ (2). Crystals were grown by slow vapor diffusion of hexane into a concentrated solution of **2** in CH_2Cl_2. A single crystal (0.18 × 0.14 × 0.14 mm) coated with Paratone-8277 was mounted on a glass fiber and immediately placed in a cold nitrogen steam at −80 °C. The X-ray intensity data were collected on a standard Siemens SMART CCD area detector system equipped with a normal focus molybdenum-target X-ray tube operated at 2.0 kW (50 kV, 40 mA). A total of 1321 frames of data (1.3 hemispheres) were collected using a narrow frame method with scan widths of 0.3° in ω and exposure times of 10 s/frame using a detector-to-crystal distance of 5.088 cm (maximum 2θ angle of 56.54°). The total data collection time was approximately 13 h. Frames were integrated with the Siemens SAINT program to 0.90 Å to yield a total of 4857 reflections, 1614 of which were independent. Crystal, data collection,[40] and refinement parameters are summarized in Table 1. The structure was solved using direct methods and refined by full-matrix least-squares on F^2. All non-hydrogen atoms were refined with anisotropic thermal parameters. Hydrogen atoms were included in idealized positions, giving a data:parameter ratio of about 11:1 in final least-squares refinements. Final refined atomic coordinates and anisotropic thermal parameters are given in the Supporting Information.

Molecular Orbital Calculations. Iterative extended Hückel (IEH) calculations were performed using the program FORTICON8.[41] The H_{ii} values obtained from valence-orbital ionization potentials (VOIP) for H, C, and N were included in the program. For Pt, the double-ζ expansion was used and the H_{ii} values were charge-iterated for square planar complexes.[42] The geometries of the complexes were optimized using PCSpartan plus,[40] giving C_{2v} symmetry for Pt(phen)(C≡$CH)_2$, Pt(phen)(C≡$CC_6H_5)_2$, and Pt(phen)(C≡$CF)_2$ and C_s symmetry for Pt(phenNO_2)(C≡$CH)_2$. The structures were optimized with Pt−N and Pt−C bond distances constrained at 1.948 and 2.062 Å, respectively, as observed for the structure of **2**.

Results and Discussion

Synthesis and Characterization. The synthetic strategy for making the complexes Pt(diimine)(C≡$CAr)_2$ shown below

(36) Kober, E. M.; Marshall, J. L.; Dressick, W. J.; Sullivan, B. P.; Caspar, J. V.; Meyer, T. J. *Inorg. Chem.* **1985**, *24*, 2755−2763.
(37) Williams, A. T. R.; Winfield, S. A.; Miller, J. N. *Analyst* **1983**, *108*, 1067−1071.
(38) Chen, L.; Farahat, M. S.; Gaillard, E. R.; Farid, S.; Whitten, D. G. *J. Photochem. Photobiol., A* **1996**, *95*, 21−25.
(39) Jukabiak, R.; Collison, C. J.; Wan, W. C.; Rothberg, L. J.; Hsieh, B. R. *J. Phys. Chem. A* **1999**, *103*, 2394−2398.
(40) Wavefunction, Inc., 18401 Von Karman, Suite 370, Irvine, CA 92612.
(41) QCPE Program No. 344, Indiana University Chemistry Department.
(42) Hoffmann, R.; Summerville, R. H. *J. Am. Chem. Soc.* **1976**, *98*, 7240−7254.

involves a CuI-catalyzed chloride-to-alkyne metathesis that has been used for synthesizing other Pt alkynyl derivatives.[43] The complexes Pt(dbbpy)(C≡$CC_6H_4X)_2$, with X = H, CH_3, OCH_3, NO_2, or F, were obtained in good yield by this strategy from stoichiometric reaction of Pt(dbbpy)Cl_2 with the corresponding terminal alkyne HC≡CC_6H_4X. For the dbbpy systems, the CuI catalyst (10 mol %) was used with dichloromethane as solvent and diisopropylamine as base. The preparation of the 5-substituted phenanthroline derivatives Pt(Rphen)(C≡$CC_6H_4X)_2$ required sonication because of low solubility of the dichloride starting compounds Pt(Rphen)Cl_2 in the dimethylformamide/diethylamine solvent/base combination employed.

All of the complexes were characterized by ^{1}H NMR, FT-IR, electronic absorption, and emission spectroscopies, mass spectrometry, and elemental analyses. The spectroscopic data support the anticipated structure assignment of a square planar coordinated platinum(II) ion with two *cis*-alkynyl ligands and a diimine chelate. The cis disposition of the alkynyl ligands leads to two bands at ca. 2100 cm^{-1} corresponding to the symmetric and asymmetric $\nu_{C\equiv C}$ stretches of the alkynyl ligands.[43] The structural assignment for the Pt(diimine)(C≡$CAr)_2$ complexes was confirmed by a structure determination of the bis(tolylacetylide) derivative Pt(phen)(C≡$CC_6H_4CH_3)_2$ (**2**). While the structure of Pt(phen)(C≡$CC_6H_5)_2$ (**1**) has been mentioned in the literature,[28] details of that determination have not yet appeared.

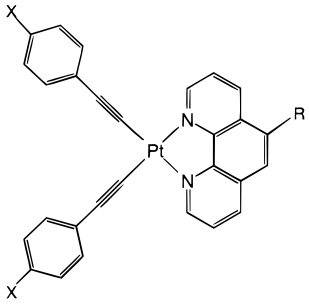

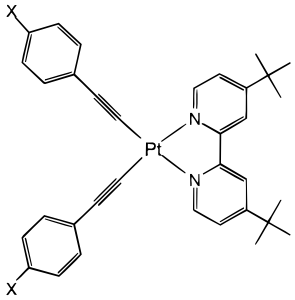

	R	X
1	H	H
2	H	Me
3	H	Me
4	NO_2	H
5	Br	H
6	Cl	H
7	Me	H
8	PhC≡C	H

	X
9	H
10	Me
11	F
12	OMe
13	NO_2

Molecular Structure of Pt(phen)(C≡$CC_6H_4CH_3)_2$ (2). The molecular structure of **2**, which is crystallographically required to have C_2 symmetry, is shown in Figure 1 along with the atom numbering scheme used. Important bond lengths and angles are given in Table 2, while a complete tabulation of distances and angles may be found in the Supporting Information. The Pt−N distance is 2.063(3) Å and compares well to those of other Pt(phen) complexes, such as [Pt(phen)$_2$]Cl_2, which exhibits a Pt−N bond length of 2.033(6) Å.[44] The Pt−C bond distance is

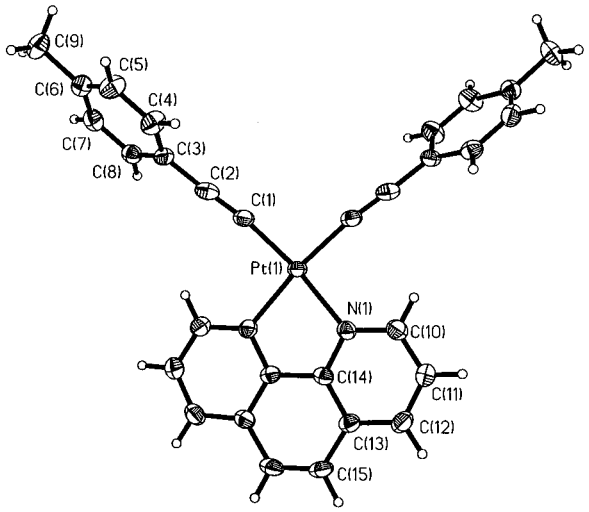

Figure 1. Molecular structure and atom numbering scheme for Pt(phen)(C≡$CC_6H_4CH_3)_2$ (**2**) (50% probability ellipsoids).

Table 2. Selected Bond Lengths (Å) and Angles (deg) for **2**[a]

Pt(1)−C(1)	1.948(3)	C(11)−C(12)	1.365(5)
Pt(1)−N(1)	2.063(3)	C(12)−C(13)	1.406(4)
N(1)−C(10)	1.347(4)	C(13)−C(14)	1.397(4)
N(1)−C(14)	1.361(4)	C(13)−C(15)	1.436(5)
C(1)−C(2)	1.201(5)	C(14)−C(14)′	1.425(6)
C(2)−C(3)	1.452(5)	C(15)−C(15)′	1.334(8)
C(10)−C(11)	1.381(5)		

C(1)′−Pt(1)−C(1)	92.5(2)	C(10)−N(1)−Pt(1)	128.1(2)
C(1)−Pt(1)−N(1)′	94.32(12)	C(14)−N(1)−Pt(1	113.6(2)
C(1)−Pt(1)−N(1)	170.83(12)	C(2)−C(1)−Pt(1)	170.4(3)
N(1)′−Pt(1)−N(1)	79.64(14)	C(1)−C(2)−C(3)	177.8(4)
C(10)−N(1)−C(14)	118.0(3)	N(1)−C(14)−C(14)′	116.5(2)

[a] Symmetry transformations used to generate equivalent (primed) atoms: $-x + 1, y, -z + 3/2$.

1.948(3) Å, which compares well with values of 2.02(4) and 1.958(7) Å for the two independent molecules of [Pt(C≡C^{t}Bu)$_4$]$_2$Ag$_4$,[45] 2.01(3) Å in [*cis*-{Pt($C_6F_6)_2$(C≡$CSiMe_3)_2$}-Pd(η^3-C_3H_5)]$^-$,[46] 2.026(9) Å in [($PPh_3)_2$Pt(μ-η^1-η^2-C≡C^{t}Bu)$_2$Pd(η^3-C_3H_5)]$^+$,[47] 1.998(4) Å in *trans*-Pt(2,2′:6′,2″-terpyridin-4′-ylethynyl)($PBu_3)_2$,[48] and 2.013(1) Å in [{*cis*-Pt($C_6F_5)_2$-(C≡$CPh)_2$}$_2$Ag$_2$]$^{2-}$.[49] Only the Pt−C distance of 2.17(2) Å found in [Pt$_2$(μ-C═CHPh)(C≡CPh)($PEt_3)_4$]$^+$ [50] is significantly longer compared to the present value. The phenanthroline ligand is planar to within 0.061 Å, while the phenyl rings are tilted at an angle of 56° from the phenanthroline plane.

Deviations from square planar coordination geometry are relatively minor. The C−Pt−C angle is 92.5(2)°, while a 9.6° twist angle exists between the PtNN and PtCC planes defined by the donor atoms. An examination of the crystal packing shown in Figure 2 reveals an intricate network containing cofacial π stacking between phenyl rings on adjacent molecules and perpendicular aromatic interactions between phenyl rings and neighboring phenanthroline ligands. The closest intermo-

(43) Sonogashira, K.; Fujikura, Y.; Yatake, T.; Toyoshima, N.; Takahashi, S.; Hagihara, N. *J. Organomet. Chem.* **1978**, *145*, 101−108.
(44) Hazell, A.; Mukhopadhyay, A. *Acta Crystallogr.* **1980**, *B36*, 1647−1649.
(45) Espinet, P.; Fornies, J.; Martinez, F.; Tomas, M.; Lalinde, E.; Moreno, M. T.; Ruiz, A.; Welch, A. J. *J. Chem. Soc., Dalton Trans.* **1990**, 791−798.
(46) Berenguer, J. R.; Fornies, J.; Lalinde, E.; Martinez, F. *J. Organomet. Chem.* **1994**, *470*, C15−C18.
(47) Berenguer, J. R.; Fornies, J.; Lalinde, E.; Martinez, F. *Organometallics* **1996**, *15*, 4537−4546.
(48) Harriman, A.; Hissler, M.; Ziessel, R.; DeCian, A.; Fisher, J. *J. Chem. Soc., Dalton Trans.* **1995**, 4067−4080.
(49) Espinet, P.; Fornies, J.; Martinez, F.; Sotes, M.; Lalinde, E.; Moreno, M. T.; Ruiz, A.; Welch, A. J. *J. Organomet. Chem.* **1991**, *403*, 253−267.

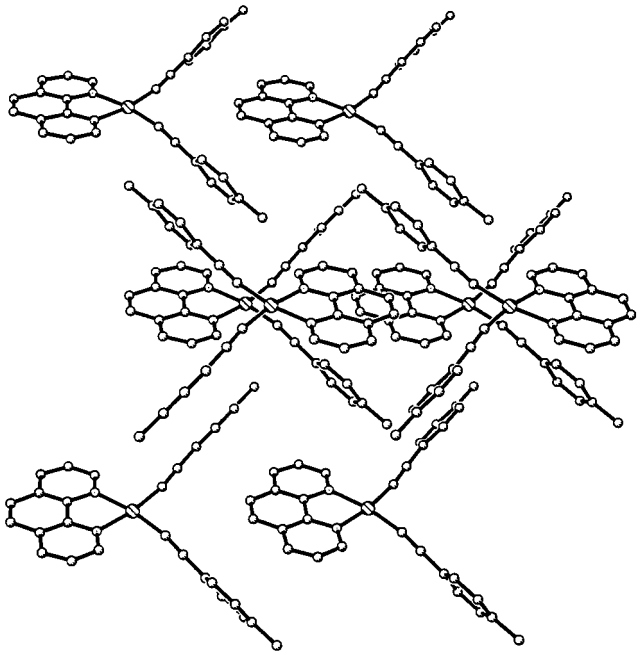

Figure 2. Packing diagram for Pt(phen)(C≡$CC_6H_4CH_3$)$_2$ (**2**). The nearest Pt···Pt distance is 5.92 Å.

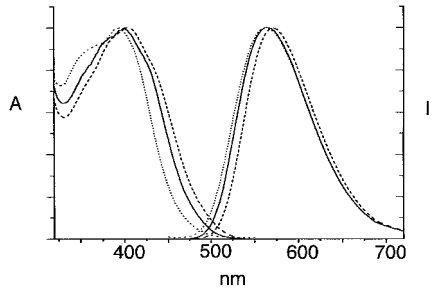

Figure 3. Normalized absorption and RT emission spectra of Pt(phen)(C≡CC_6H_5)$_2$ in CH_2Cl_2 (—), acetonitrile (···), and 2:1 Et_2O/CH_2Cl_2 (- - -).

lecular contact of the former type is between C7 and C7′ at 3.20 Å, and that of the latter type is between C5 and C12′ at 3.48 Å. The closest Pt···Pt contact is 5.92 Å, indicating the absence of any interaction between metal centers.

Absorption Spectra. The absorption spectra of the complexes exhibit a slightly solvatochromic band near 400 nm, as shown in Figure 3 for **1**, in addition to higher energy bands (λ < 310 nm) that correspond to diimine- and acetylide-based intraligand transitions. The slightly solvatochromic transition with a molar extinction coefficient ϵ of ca. 8000 M^{-1} cm^{-1} has been assigned by Che as a charge-transfer excitation from a filled metal d orbital to a vacant $\pi^*_{diimine}$ orbital (MLCT).[28] The dependence of this absorption maximum on the diimine and acetylide substituents has been studied for both series of complexes, and these results are tabulated in Table 3 and illustrated in Figure 4. Interpretation of these spectra is complicated by the fact that this asymmetric band clearly is comprised of more than one transition. In fact, a higher energy shoulder (350−370 nm) is resolved in absorption spectra of **1**, **5**, **6**, and **7** (Figure 4A). This shoulder shifts strongly to lower energy as the electron-withdrawing properties of the substituent on the phenanthroline ligand increase (CH_3, H, ∼350 nm; Cl, ∼370 nm); for the NO_2-phen complex **4**, this feature presumably is buried in the 400 nm band envelope. In contrast, the absorption *maximum* for the Pt(Rphen)(C≡CPh)$_2$ series shows only a modest shift from 392 nm for **1** to 397 nm for **4** as the phenanthroline substituent is varied. Nevertheless, it is evident that the aggregate transitions comprising the 400 nm band shift to lower energy as the electron-accepting properties of the phenanthroline increase. In particular, it is striking that the low-energy tail of this absorption manifold systematically shifts to lower energy as the electron-withdrawing properties of the diimine substituents increase (Me < H < Cl, Br < NO_2).[51] This behavior is entirely consistent with charge transfer to diimine transitions.

The influence of varying the para substituent of the arylacetylide ligands on the ca. 400 nm feature is shown in Figure 4B. While the difference in absorption maxima is nearly indiscernible for X = H and F, the band does exhibit a significant shift to lower energy for X = OCH_3 and CH_3. Moreover, it is noteworthy that the low-energy tail of the absorption manifold systematically shifts to lower energy as the electron-donating properties of the acetylide substituents increase (F < H < Me < OCH_3). These results are consistent with the notion that the HOMO is predominantly metal-based. As arylacetylide donicity increases, it is expected that the energies of nonbonding and weakly π bonding metal orbitals will increase,[18] leading to the observed red shifts for the Pt(dbbpy)(C≡$CC_6H_4OCH_3$)$_2$ (**11**) and Pt(dbbpy)(C≡$CC_6H_4CH_3$)$_2$ (**10**) derivatives.

The *p*-nitrophenylacetylide complex Pt(dbbpy)(C≡$CC_6H_4NO_2$)$_2$ (**13**) exhibits an absorption spectrum that is significantly different from those of the rest of the series and is omitted from Figure 4B. Specifically, the lowest energy absorption band, which is significantly blue shifted, possesses a molar extinction coefficient that is substantially higher ($\epsilon \sim 37\,000$ M^{-1} cm^{-1}) than those of the rest of the series. While the shift of the MLCT absorption to higher energy (ca. 380 nm) is expected for the nitro derivative **13** on the basis of reduced donor ability for the acetylide ligands, the change in molar absorptivity suggests that the observed band actually corresponds to a different transition, obscuring the MLCT band. The intense 380 nm absorption is attributed to a transition based on the *p*-nitrophenylacetylide ligand. Free *p*-$NO_2C_6H_4C$≡CH exhibits a similar band at 286 nm that shifts to lower energy upon coordination. Support for this notion is seen in the electrochemical results discussed below.

Emission Spectra. Figure 5 presents the room temperature and 77 K emission spectra of Pt(dbbpy)(C≡CC_6H_5)$_2$ (**9**) and Pt(CH_3phen)(C≡CC_6H_5)$_2$ (**7**) as well as their absorption spectra. The room-temperature emission is broad and asymmetric, while the 77 K spectrum in butyronitrile glass shows a rigidochromic shift and resolvable vibronic components of the emission. The room-temperature luminescence mirrors the absorption spectrum with good 0−0 overlap. For the 77 K spectrum, the vibronic interval is ∼1230 cm^{-1}, which is diagnostic of diimine involvement in the emissive excited state, and the Huang−Rhys constant *S*, $I(1,0)/I(0,0)$, is about 0.65 and 0.90 for **7** and **9**, respectively. The latter compares to values of 1.4 observed for the ^{3}IL emission of the Pt(bpy)(en)$^{2+}$ cation[17] and slightly greater than 1 observed for the solid-state emission of Pt(3,3′-(CH_3-OCO)$_2$bpy)Cl_2.[18]

The influence of substituent variation on the emission energies for the Pt(Rphen)(C≡CC_6H_5)$_2$ and Pt(dbbpy)(C≡CC_6H_4X)$_2$ series of complexes is shown in Figure 6 and tabulated in Table 3. The extent of the observed shifts is greater than those seen

(50) Afzal, D.; Lenhert, P. G.; Lukehart, C. M. *J. Am. Chem. Soc.* **1984**, *106*, 3050−3052.

(51) In Figure 4, panel A, the Brphen complex **5** is omitted for clarity since it and the Clphen derivative **6** have very similar absorption spectra as would be expected on the basis of the similar electron-withdrawing ability of the chloro and bromo substituents.

Table 3. Absorption Maxima, Emission Maxima, Luminescence Quantum Yields, Excited-State Lifetimes, and Self-Quenching Rate Constants for Pt(diimine)($C{\equiv}CAr)_2$ Complexes in Acetonitrile

compound	λ_{abs} (nm)	λ_{em} (nm)	ϕ_{em}[a]	τ_o (ns)[b]	k_q ($\times 10^9$ s^{-1})
Pt(phen)($C{\equiv}CC_6H_3)_2$ (**1**)	392 (8000)	575	0.090	907[c]	6.3[c]
Pt(phen)($C{\equiv}CC_6H_4CH_3)_2$ (**2**)	392 (9800)	578		549[c]	6.2[c]
Pt(phen)($C{\equiv}CC_6H_4F)_2$ (**3**)	391 (7100)	584		814[c]	6.7[c]
Pt(NO_2phen)($C{\equiv}CC_6H_5)_2$ (**4**)	397 (5000)	582	0.003	~400	
Pt(Brphen)($C{\equiv}CC_6H_5)_2$ (**5**)	395 (8000)	605	0.036	366	4.6 + 0.2
Pt(Clphen)($C{\equiv}CC_6H_5)_2$ (**6**)	397 (7200)	605	0.040	390	5.5 ± 0.7
Pt(CH_3phen)($C{\equiv}CC_6H_5)_2$ (**7**)	396 (7600)	575	0.098	972	5.5 ± 0.2
Pt($C_6H_5C{\equiv}$Cphen)($C{\equiv}CC_6H_5)_2$ (**8**)	396 (9600)	590[e]		5600	4.2 ± 0.3
Pt(dbbpy)($C{\equiv}CC_6H_5)_2$ (**9**)	386 (7900)	570	0.11	691	1.4 ± 0.2
Pt(dbbpy)($C{\equiv}CC_6H_4CH_3)_2$ (**10**)	389 (8200)	592	0.07	440	1.0 ± 0.2
Pt(dbbpy)($C{\equiv}CC_6H_4OCH_3)_2$ (**11**)	393 (6600)	640	0.002	14[d]	
Pt(dbbpy)($C{\equiv}CC_6H_4{-}F)_2$ (**12**)	385 (7500)	570	0.14	663	1.6 ± 0.1
Pt(dbbpy)($C{\equiv}CC_6H_4{-}NO_2)_2$ (**13**)	371 (38100)	570	0.04	~4500	

[a] Luminescence quantum yields are extrapolated to infinite dilution. Estimated error is ±15%. [b] τ_o is the lifetime at infinite dilution ± 5%. [c] Measured in acetonitrile (ref 30). [d] Measured by single-photon counting at one concentration (2.9×10^{-5} M). [e] There is a shoulder to higher energy.

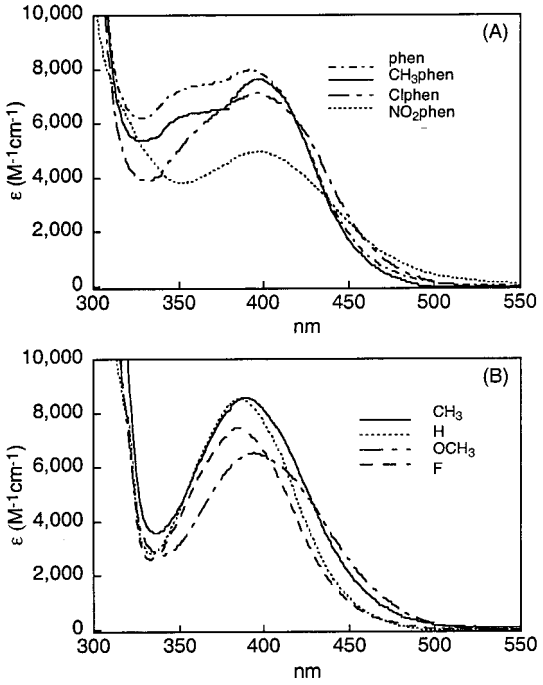

Figure 4. Absorption spectra for the Pt(Rphen)($C{\equiv}CC_6H_5)_2$ series (A) and Pt(dbbpy)($C{\equiv}CC_6H_4X)_2$ series (B) in CH_3CN at room temperature.

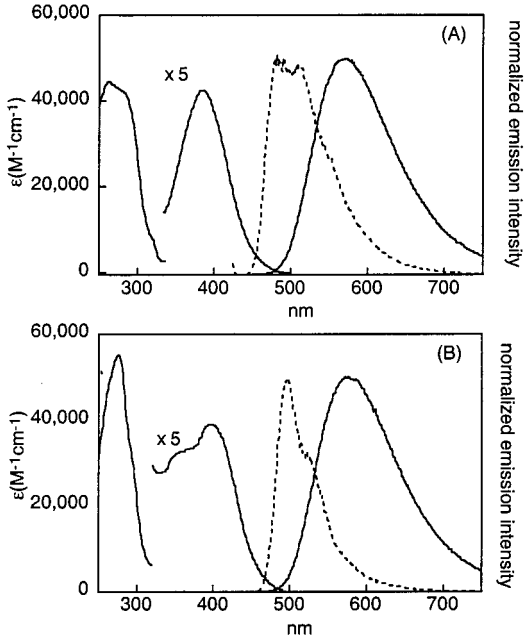

Figure 5. Absorption and emission spectra at room temperature in CH_3CN (—) and 77 K emission spectra in butyronitrile (- - -) for (A) Pt(dbbpy)($C{\equiv}CC_6H_5)_2$ (**9**) and (B) Pt(CH_3phen)($C{\equiv}CC_6H_5)_2$ (**7**).

in the absorption spectra of Figure 4 with trends that are exactly parallel. Shifts to lower energy in emission bands occur as the electron-withdrawing ability of the diimine substituent increases and as the donicity of the arylacetylide ligand increases. Both changes are consistent with a mainly metal-based HOMO and a $\pi^*_{diimine}$ LUMO. The influence of substituent variation on the emission energies for the Pt(Rphen)($C{\equiv}CC_6H_5)_2$ and Pt(dbbpy)-($C{\equiv}CC_6H_4X)_2$ series of complexes is shown in Figure 6 and tabulated in Table 3. The extent of the observed shifts is greater than those seen for the ca. 400 nm absorption maximum with trends that are exactly parallel. The emission maximum shifts to lower energy as the electron-withdrawing ability of the diimine substituent increases and as the donicity of the aryl-acetylide ligands increases. This behavior is consistent with a mainly metal-based HOMO and a $\pi^*_{diimine}$ LUMO. From the limited data set tested, the HOMO−LUMO gap appears to be much more sensitive to substitution on the diimine than on the aryl group of the alkynyl ligands; the relative insensitivity to para substituents of the arylacetylide ligands is in keeping with their distance from the predominantly metal-centered HOMO and diimine-centered LUMO. More dramatic perturbations in the emission are realized when the acetylide ligands are replaced with other carbanion ligands, namely, phenyl or methyl groups. Figure 7 shows the 77 K ethanol/methanol (3:1) glass emission spectra for a series of Pt(phen)R_2 complexes where R is $C{\equiv}CC_6H_5$, C_6H_5, or CH_3. The emissions from the methyl[52] and aryl[53] derivatives previously have been identified as originating from lowest ^{3}MLCT excited states. The onset of the ^{3}MLCT emission from the Pt(phen)($C{\equiv}CC_6H_5)_2$ occurs ca. 400 and 1000 cm^{-1} to higher energy of the onset of the emission from the phenyl and methyl complexes, respectively. It is striking that the energy of the onset of emission from these complexes decreases ($C{\equiv}CC_6H_5 > C_6H_5 > CH_3$) with increasing basicity of the carbanion ligands ($sp < sp^2 < sp^3$). These observations are consistent with more electron-donating ligands stabilizing MLCT states as discussed by Miskowski and coworkers.[18]

(52) Hill, R. H.; Puddephatt, R. J. *J. Am. Chem. Soc.* **1985**, *107*, 1219−1225.
(53) Klein, A.; Kaim, W. *Organometallics* **1995**, *14*, 1176−1186.

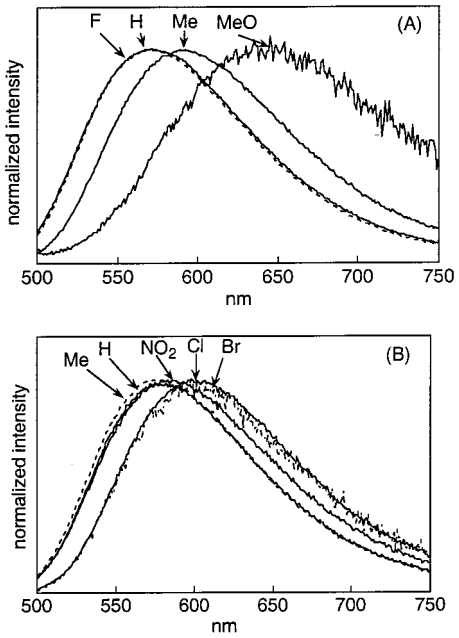

Figure 6. Normalized emission spectra for the Pt(Rphen)(C≡CC_6H_5)$_2$ series (A) and Pt(dbbpy)(C≡CC_6H_4X)$_2$ series (B) in CH_3CN at room temperature.

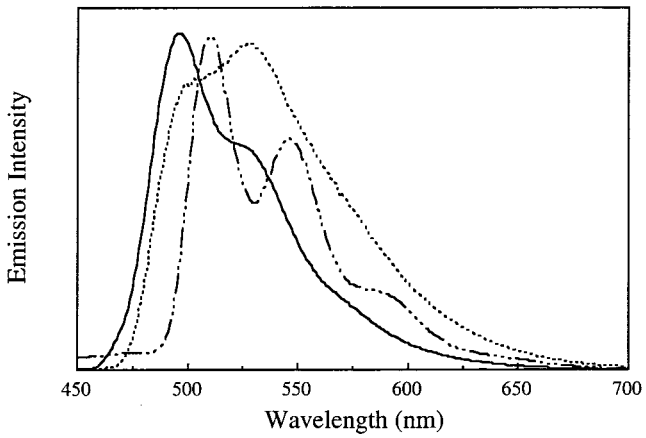

Figure 7. Emission spectra (77 K) of Pt(phen)R_2 in ethanol/methanol (3:1) glass where R is C≡CC_6H_5 (—), C_6H_5 (···), and CH_3 (—···—).

IEH molecular orbital calculations also support the assignment of the emission to a lowest ^{3}MLCT excited state. As shown in Table 4, the HOMO is primarily metal d_σ in character and the LUMO is localized on the phenanthroline ligand. The HOMO−LUMO gaps obtained for Pt(phen)(C≡CC_6H_5)$_2$, Pt(phen)(C≡CH)$_2$, Pt(phen)(C≡CF)$_2$, and Pt(phenNO_2)(C≡CH)$_2$ are 1.59, 1.65, 1.70, and 0.76 eV, respectively. This trend is consistent with that observed for the low-energy MLCT absorptions at ca. 400 nm and for the room-temperature emission at ca. 580 nm in MeCN solution for the Pt(dbbpy)(C≡CC_6H_4X)$_2$ series of complexes. The fact that the calculated HOMO−LUMO gap is at least 0.7 eV less energetic than the observed emission energies indicates that these calculations are of value mainly in the comparison of electronically similar systems and not in any absolute sense.

Whereas all of the emission spectra presented in Figure 6 show one asymmetric but structureless band, the emission spectrum of **8** gives evidence of a vibrational progression with a Huang−Rhys parameter of greater than 1 and, at higher concentrations, of a substantially red-shifted emission at 750 nm. The emission spectrum for **8** in MeCN solutions at two different concentrations is shown in Figure 8. The red-shifted emission at higher concentration is assigned as an excimer emission consistent with what has been described by Connick et al. for Pt(phen)(C≡CC_6H_5)$_2$ (**1**) and by Vogler and Che for the di(cyanide) derivatives.[19,20,30]

Electrochemistry. Cyclic voltammograms recorded for the Pt(diimine)(C≡CAr)$_2$ complexes all exhibit one reversible reduction wave between −1.20 and −1.50 V, corresponding to the addition of an electron to an orbital on the respective diimine ligand (Table 5).[54] Substitution at the 5-position of phenanthroline while keeping the alkynyl ligand fixed (**1**, **5**−**7**) has a more substantial effect on the $E_{1/2}$ reduction potentials than does a corresponding variation of the arylacetylide substituent while keeping the diimine fixed (**9**−**12**). For the former series, methyl substitution at the 5-position makes the reduction more difficult while chloro, bromo, and phenylethynyl substituents shift $E_{1/2}$ very modestly to less negative values. Substitution at the 5-position of phenanthroline clearly influences the energy of the π^*_{diimine} LUMO, which is in turn probed by one-electron reduction. The phenylethynyl substituent in **8** may achieve this effect through greater delocalization.

The compounds containing nitro groups (**4** and **13**) exhibit additional reduction waves that are not observed in the cyclic voltammograms of the other complexes. On the basis of the electrochemical behavior of the free ligands,[55a] these waves are attributed to nitro group reductions. For both NO_2phen and *p*-$NO_2C_6H_4C$≡C ligands, the observed $ArNO_2$-based reduction waves occur at more positive values when coordinated to Pt than when not coordinated, as expected on the basis of donation of electron density upon coordination. Further support for assigning the additional, less cathodic reduction waves to the nitro groups is obtained from the electrochemical study of the related Pt(4,4′-$(NO_2)_2$bpy)Cl_2 complex, which shows facile reductions that are highly localized on the nitro groups.[55b] The shift in reduction potential between **13** and free *p*-nitrophenylacetylene is completely consistent with the observed shift in their absorption spectra for the intense low-energy band. The 380 nm absorption band in **13** is based on *p*-nitrophenylacetylide, and it is red-shifted relative to that of free ligand with a higher energy LUMO. This is the orbital that serves as the acceptor function upon one electrochemical reduction.

Oxidation of the Pt(diimine)(C≡CAr)$_2$ complexes is not observed in most cases up to 1.6 V vs NHE. When it is seen, the oxidation wave is irreversible. The results can be compared with previous reports on platinum diimine dithiolate systems and other Pt complexes containing heteroaromatic or related chelating ligands that show only irreversible oxidations.[23,56−58]

Excited-State Lifetimes and Emission Quantum Yields. In Table 3 are presented the lifetimes at infinite dilution (τ_o) and the self-quenching rate constants (k_q) for all of the compounds studied except the nitro-containing derivatives **4** and **13**. These two compounds were too weakly emissive to be analyzed by the same procedure as done for the rest of the compounds (i.e., similar concentration ranges and excitation power per pulse). The methoxyphenylacetylide compound **11** is also weakly emissive ($\phi_{em} = 0.002$). While its short excited-state lifetime was measured by single-photon counting (∼14 ns in a 2.9×10^{-5} M acetonitrile solution), a quenching study

(54) Ohsawa, K. W.; Hanck, K. W.; DeArmond, M. K. *J. Electroanal. Chem. Interfacial Electrochem.* **1984**, *175*, 229−240.
(55) (a) Bock, C. R.; Connor, J. A.; Gutierrez, A. R.; Meyer, T. J.; Whitten, D. G.; Sullivan, B. P.; Nagle, J. K. *J. Am. Chem. Soc.* **1979**, *101*, 4815−4824. (b) McInnes, E. J. L.; Welch, A. J.; Yellowlees, L. J. *Chem. Commun.* **1996**, 2393−2394.

Table 4. Relative Percent Atomic Contribution to the MOs

Pt(phen)(C≡CH)$_2$, C_{2v} symmetry				Pt(phenNO$_2$)(C≡CH)$_2$, C_s symmetry				
energy of MO, eV	Pt	C≡C	phen π	energy of MO, eV	Pt	C≡C	phen π	NO_2
−7.45	0.1	0.2	99.7	−7.57	16.2	71.7	12.1	0.0
−7.57	16.5	72.8	10.7	−8.07	1.8	4.0	93.0	1.2
−8.11	1.5	3.5	95.0	−9.31	0.3	0.1	83.0	16.6
−9.60	0.3	0.1	99.6	−9.73	2.1	1.1	96.7	0.0
−9.73	2.2	1.2	96.7	−10.62	0.1	0.0	32.7	67.3
−11.38	61.7	8.4	0.0	−11.38	61.3	8.4	28.2	0.3
−12.16	17.7	4.2	78.1	−12.22	66.7	25.4	7.1	0.1
−12.22	66.9	25.5	0.0	−12.25	31.8	7.6	54.2	6.4
−12.33	61.7	15.0	23.3	−12.34	63.0	15.3	21.3	0.4
−12.47	59.6	15.5	24.9	−12.49	20.0	5.2	60.6	8.4
−12.52	21.1	5.2	0.0	−12.51	45.2	12.1	38.4	4.3

Pt(phen)(C≡CPh)$_2$, C_{2v} symmetry				Pt(phen)(C≡CF)$_2$, C_{2v} symmetry				
energy of MO, eV	Pt	C≡C	phen π	energy of MO, eV	Pt	C≡C	phen π	2F
−8.27	0.0	0.0	0.0	−7.4	46.3	24.5	27.8	1.0
−8.71	0.2	25.4	0.5	−7.4	0.1	0.1	99.8	0.0
−8.77	3.3	26.1	0.1	−8.1	1.1	1.5	97.4	0.1
−9.52	0.8	0.1	99.1	−9.6	0.3	0.1	99.6	0.0
−9.82	2.5	0.9	96.5	−9.7	2.2	0.9	96.8	0.1
−11.41[a]	65.3	10.9	20.7	−11.4[a]	61.8	6.1	30.3	0.3
−11.93	50.6	21.6	3.2	−12.1	65.5	27.3	4.6	2.3
−12.16	56.0	21.5	16.4	−12.1	23.5	6.5	69.5	0.5
−12.16	46.0	17.0	32.1	−12.3	62.1	19.5	16.8	1.6
−12.27	0.5	37.8	1.7	−12.4	50.0	16.4	32.3	1.3
−12.42	16.8	8.4	71.9	−12.5	21.3	3.0	68.5	0.2

[a] Highest occupied molecular orbital.

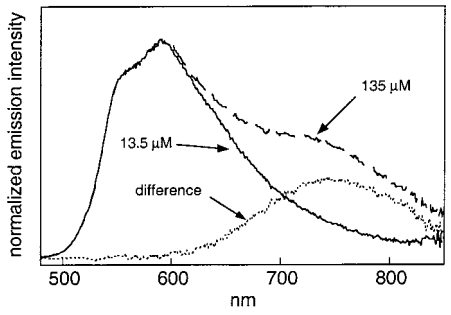

Figure 8. Normalized emission spectra of Pt(C_6H_5C≡Cphen)-(C≡CC_6H_5)$_2$ (**8**) at 135 and 13.5 μM. The difference between these spectra is also shown (···).

was not performed. Because the measurement was made at low concentration, there is an insignificant deviation from the measured lifetime compared to a value that might be extrapolated to infinite dilution.[59]

Table 3 shows that some of the systems have luminescence quantum yields nearly twice that of Ru(bpy)$_3^{2+}$ in acetonitrile. Luminescent quantum yields in Table 3 were corrected for infinite dilution using a modified Stern−Volmer equation[60] (eq 3), where ϕ and ϕ_o are the measured quantum yield and the quantum yield at infinite dilution, respectively.

$$\phi_o/\phi = 1 + k_q\tau_o[\mathrm{Pt}] \quad (3)$$

From the lifetime and emission quantum yields, the radiative and nonradiative rate constants can be calculated using eqs 4 and 5.

Table 5. Electrochemical Data ($E_{1/2}$ Values for Reductions and Irreversible Oxidation Waves) for Pt(diimine)(C≡CAr)$_2$ Complexes

compound	E_{ox} (V)	E_{red} (V)
Pt(phen)(C≡CC_6H_5)$_2$ **(1)**[a]		−1.31, −2.00
Pt(phen)(C≡$CC_6H_4CH_3$)$_2$ **(2)**[a]		−1.30
Pt(phen)(C≡CC_6H_4F)$_2$ **(3)**[b]		−1.29
Pt(NO_2phen)(C≡CC_6H_5)$_2$ **(4)**[a]		−0.62, −0.89, −1.36
Pt(Brphen)(C≡CC_6H_5)$_2$ **(5)**[a]		−1.17
Pt(Clphen)(C≡CC_6H_5)$_2$ **(6)**[b]		−1.20
Pt(CH_3phen)(C≡CC_6H_5)$_2$ **(7)**[b]	1.15 (irr)	−1.41
Pt(dbbpy)(C≡CC_6H_5)$_2$ **(9)**[b]		−1.40
Pt(dbbpy)(C≡$CC_6H_4CH_3$)$_2$ **(10)**[b]	1.18 (irr)	−1.42
Pt(dbbpy)(C≡$CC_6H_4OCH_3$)$_2$ **(11)**[b]	1.02 (irr)	−1.42
Pt(dbbpy)(C≡$CC_6H_4NO_2$)$_2$ **(13)**[c]		−0.95, −1.20, −1.53
Pt(dbbpy)(C≡CC_6H_4F)$_2$ **(12)**[b]		−1.39
Pt(C_6H_5C≡Cphen)(C≡CC_6H_5)$_2$ **(8)**[b]		−1.21
p-NO_2-C_6H_4−C≡CH		−1.07
5-nitrophenantroline[a]		−0.96, −1.67

[a] In dimethylformamide solution containing 0.1 M (TBA)PF_6 at 293 K. [b] In acetonitrile solution containing 0.1 M (TBA)PF_6 at 293 K. [c] In dichloromethane solution containing 0.1 M (TBA)PF_6 at 293 K. Potentials in volts are versus NHE as calibrated using the ferrocene/ferrocenium couple at 0.40 V vs NHE (see the Experimental Section).

$$k_r = \phi_o\tau_o^{-1} \quad (4)$$

$$k_{nr} = k_r(\phi_o^{-1} - 1) \quad (5)$$

In Table 6 are shown E_{em}^{max}, k_r, and k_{nr} for the Pt(Rphen)-(C≡CC_6H_5)$_2$ and Pt(dbbpy)(C≡CC_6H_4X)$_2$ series. The radiative

(56) Zuleta, J. A.; Burberry, M. S.; Eisenberg, R. *Coord. Chem. Rev.* **1990**, *97*, 47−64.
(57) Cornioley-Deuschel, C.; von Zelewsky, A. *Inorg. Chem.* **1987**, *26*, 3354−3358.
(58) Blanton, C. B.; Murtaza, Z.; Shaver, R. J.; Rillema, D. P. *Inorg. Chem.* **1992**, *31*, 3230−3235.

(59) If one assumes that the self-quenching constant for compound **11** is similar to those of the rest of the compounds in the Pt(dbbpy)-(C≡CC_6H_4X)$_2$ series obtained from eq 2, it can be seen that the difference in τ vs τ_o is less than 0.1%. Compared to the estimated error of 5% in the value of τ_o, this error is negligible. Likewise, the correction for the quantum yield at infinite dilution will be negligible too.

(60) Vincze, L.; Sandor, F.; Pem, J.; Bosnyak, G. *J. Photochem. Photobiol. A* **1999**, *120*, 11−14.

Table 6. Radiative and Nonradiative Rates for the Pt(Rphen)(C≡CPh)$_2$ and Pt(dbbpy)(C≡CC$_6$H$_4$X)$_2$ Series[a]

compound	E_{em}^{max} (cm^{-1})	k_r ($\times 10^6$ s^{-1})	k ($\times 10^6$ s^{-1})	k_{nr} ($\times 10^6$ s^{-1})
Pt(phen)(C≡CC$_6$H$_5$)$_2$ **(1)**	17 300	0.099	1.103	1.00
Pt(NO$_2$phen)(C≡CC$_6$H$_5$)$_2$ **(4)**	17 180	0.008	2.500	2.49
Pt(Brphen)(C≡CC$_6$H$_5$)$_2$ **(5)**	16 530	0.129	3.497	3.37
Pt(Clphen)(C≡CC$_6$H$_5$)$_2$ **(6)**	16 530	0.103	2.564	2.46
Pt(CH$_3$phen)(C≡CC$_6$H$_5$)$_2$ **(7)**	17 390	0.101	1.029	0.93
Pt(dbbpy)(C≡CC$_6$H$_5$)$_2$ **(9)**	17 540	0.159	1.447	1.29
Pt(dbbpy)(C≡CC$_6$H$_4$CH$_3$)$_2$ **(10)**	16 890	0.159	2.273	2.11
Pt(dbbpy)(C≡CC$_6$H$_4$OCH$_3$)$_2$ **(11)**	15 630	0.143	71.429	71.3
Pt(dbbpy)(C≡CC$_6$H$_4$F)$_2$ **(12)**	17 540	0.211	1.508	1.23
Pt(dbbpy)(C≡CC$_6$H$_4$NO$_2$)$_2$ **(13)**	17 540	0.007	0.177	0.17

[a] All rates are estimated to have an error of ±15%.

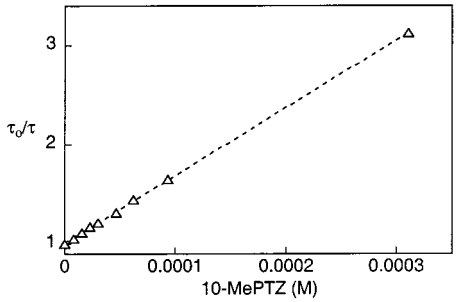

Figure 9. Stern−Volmer plot for the quenching of Pt(dbbpy)(C≡CC$_6$H$_5$)$_2$ (**9**) in CH$_3$CN with 10-methylphenothiazine.

rate constants (10^3−10^5 s^{-1}) indicate that the observed emission has a a significant degree of spin-forbiddedness consistent with a ^{3}MLCT assignment. Except for the nitro compounds **4** and **13**, all of the compounds obey the energy gap law from plots of log k_{nr} versus E_{em}^{max} for each series. This includes the short lifetime and low emission quantum yield for the electron-donating *p*-MeOC$_6$H$_4$ acetylide derivative **11**. These results lend support to the assertion that the lowest energy excited state in all of these complexes originates from a metal-to-diimine ligand charge-transfer transition.

The photophysical, electrochemical, and spectroscopic data for Pt(dbbpy)(C≡CC$_6$H$_4$NO$_2$)$_2$ (**13**) suggest that the emission from this complex originates from a different lowest excited state (involving a LUMO centered on the acetylide ligand) than observed for the other complexes in the Pt(dbbpy)(C≡C(C$_6$H$_4$-X)$_2$ series. Further spectroscopic studies on this system are in progress.

Estimation of Excited-State Reduction Potentials. The Pt(diimine)(C≡CAr)$_2$ complexes undergo electron-transfer quenching of both reductive and oxidative types. As with the corresponding diimine dithiolate complexes,[23] the systems are relatively photostable in the presence of an electron donor, whereas photodegradation occurs under oxidative quenching. For example, photolysis of Pt(dbbpy)(C≡CC$_6$C$_4$CH$_3$)$_2$ (**10**) in acetonitrile containing *p*-nitrobenzaldehyde with Hg(Xe) irradiation (λ_{ex} > 345 nm) leads to substantial photodegradation after 30 min.

For the complex Pt(dbbpy)(C≡CC$_6$H$_5$)$_2$ (**9**), reductive quenching was examined quantitatively by measuring the emission lifetime in the presence of the electron donors 10-methylphenothiazine and *N*,*N*,*N*′,*N*′-tetramethylbenzidine. Stern−Volmer behavior was observed using both quenchers with essentially diffusion-controlled k_q values of 9.6×10^9 and 1.3×10^{10} M^{-1} s^{-1}, respectively, and τ_o of 715 ± 20 ns. A plot of τ_o/τ vs the concentration of 10-methylphenothiazine is shown in Figure 9.

Through the use of a simple thermochemical cycle involving the excited-state energies E_{oo} (estimated from the 77 K emission spectra) and the reversible reduction potentials $E_{1/2}$, the excited-state *reduction* potentials for the Pt(diimine)(C≡CAr)$_2$ complexes have been estimated. Table 7 presents these results. As expected for a lowest MLCT excited state, the smallest E(Pt*/Pt$^-$) value for the Pt(Rphen)(C≡CC$_6$H$_5$)$_2$ series occurs for the complex which has an electron-donating CH$_3$ substituent on the phenanthroline ligand. Likewise, the smallest E(Pt*/Pt$^-$) value for the Pt(dbbpy)(C≡CC$_6$H$_4$X)$_2$ series occurs for complex **11**, which has an electron-donating methoxy substituent on each arylacetylide ligand. The observed ordering is consistent with the notion that the excited-state reduction potential reflects the driving force for filling the vacancy in the ground-state HOMO. A better donating ligand will increase electron density on the metal center more, thereby raising in energy the predominantly metal-centered HOMO, while shifting the excited-state reduction potential to less positive values.

Table 7. Ground- and Excited-State Redox Properties of Pt(diimine)(C≡CAr)$_2$ Complexes[a]

compound	E_{oo} (eV)	$E_{1/2}$ (red, V vs NHE)	E(Pt*/Pt$^-$)
Pt(phen)(C≡CC$_6$H$_5$)$_2$ **(1)**	2.50	−1.31	1.19
Pt(Brphen)(C≡CC$_6$H$_5$)$_2$ **(5)**	2.44	−1.17	1.27
Pt(Clphen)(C≡CC$_6$H$_5$)$_2$ **(6)**	2.44	−1.20	1.24
Pt(CH$_3$phen)(C≡CC$_6$H$_5$)$_2$ **(7)**	2.50	−1.41	1.09
Pt(dbbpy)(C≡CC$_6$H$_5$)$_2$ **(9)**	2.55	−1.38	1.17
Pt(dbbpy)(C≡CC$_6$H$_5$CH$_3$)$_2$ **(10)**	2.52	−1.37	1.15
Pt(dbbpy)(C≡CC$_6$H$_4$OCH$_3$)$_2$ **(11)**	2.38	−1.39	0.99
Pt(dbbpy)(C≡CC$_6$H$_4$F)$_2$ **(12)**	2.55	−1.36	1.19

[a] All potentials in volts vs NHE.

Conclusions

The Pt(diimine)(C≡CAr)$_2$ complexes comprise a new and potentially useful set of solution luminescent square planar complexes, with some members exhibiting greater emission intensity than comparable solutions of Ru(bpy)$_3^{2+}$. The nature of the excited state in these systems has been investigated through systematic ligand variation and its influence on excited-state properties. In this context, two series of complexes were synthesized and studied, one having the diimine held constant as di-*tert*-butylbipyridine while the para substituent on the arylacetylide ligand was changed and the other having the alkynyl fixed as phenylacetylide with the diimine varying. Through this investigation the emitting state is confirmed to be a Pt-to-diimine charge transfer in accord with that originally proposed by Che. This assignment is consistent with the notion that variation of the diimine affects the energy of the lowest unoccupied molecular orbital, and that variation of the arylacetylide leads to only minor changes in the Pt-based HOMO. Luminescence decay measurements reveal excited-state lifetimes between 14 and 5600 ns and a degree of spin-forbiddenness corresponding to a ^{3}MLCT assignment.[28] Unlike the octahedral

d^6 diimine complexes such as $Ru(diimine)_3^{2+}$ and $Re(diimine)(CO)_3X$ (where X = halide or pyridyl group),[61] these square planar d^8 complexes exhibit self-quenching of their excited state.

The $Pt(diimine)(C{\equiv}CAr)_2$ complexes undergo electron-transfer quenching with good Stern−Volmer behavior seen for $Pt(phen)(C{\equiv}CC_6H_5)_2$ when quenched by the electron donors 10-methylphenothiazine and *N*,*N*,*N*′,*N*′-tetramethylbenzidine. A simple thermochemical analysis leads to estimates for the excited-state reduction potentials in the range of ca. 1.0−1.3 V. The long-lived excited states of the $Pt(diimine)(C{\equiv}CAr)_2$ complexes, their redox properties, and the synthetic flexibility which these systems offer make these complexes very attractive for application in molecular photochemical devices and the construction of multicomponent molecular systems.

Acknowledgment. This research was supported by the Department of Energy, Division of Basic Chemical Sciences (R.E.), and the Research Corporation (D.K.G.). We thank Dr. Witek Paw and Dr. Adnan Mansour for valuable discussions, Dr. Gary Dombrowski for expert technical assistance, and Dr. Chris Collison for assistance with single-photon counting measurements.

Supporting Information Available: Tables giving crystal data and structure refinement, atomic and hydrogen coordinates, isotropic and anisotropic displacement parameters, and bond lengths and angles for **2**. This material is available free of charge via the Internet at http://pubs.acs.org.

IC991250N

(61) Roundhill, D. M. In *Photochemistry and Photophysics of Metal Complexes*; Fackler, J. P. J., Ed.; Plenum Press: New York, 1994; p 356.